Traffic & Transportation

An Activity-Journey-Network Approach for Modelling Travel Behaviour of Multiple User Classes Under Time Constraints

Lian Qun OUYANG[1], Di HUANG[2], Ling Ling XIAO[3]

Original Scientific Paper
Submitted: 6 February 2024
Accepted: 10 January 2025

[1] lillian_auyueng@163.com, College of E-Commerce, Tangshan University, Tangshan, China
[2] Corresponding author, huangd@bjtu.edu.cn, School of Economics and Management, Beijing Jiaotong University, Beijing, China
[3] lxiao@bjtu.edu.cn, School of Economics and Management, Beijing Jiaotong University, Beijing, China

Publisher:
Faculty of Transport and Traffic Sciences, University of Zagreb

ABSTRACT

The flow pattern on a given transportation network at a given moment results from many users' travel decisions which are made for some purposes, for example, participating in necessary activities such as work, eating and shopping. Consequently, the explicit modelling of the interaction between users' activity and travel choice behaviour serves as a basic building block for long-term transportation planning and management. In this paper, an activity-based network user equilibrium model is proposed to study the dynamic activity-travel scheduling problem with multiple classes of users under time constraints. A simple supernetwork representation approach is introduced to generate the activity-journey-network (AJN) which expands the basic transportation network in both time and space dimensions. With the supernetwork representation, the dynamic activity-travel scheduling problem is transformed into a static network flow assignment problem. A heuristic algorithm is developed to find the path with the maximum utility in the AJN from the start node to the end node for each user. A numerical study is conducted to illustrate the application of the proposed model and solution algorithm for several transportation networks including large-scale real-world networks. It is shown that both the individual's travel choice and group travel behaviour in a transportation network can be well studied by the proposed model.

KEYWORDS

activity-travel scheduling; activity journey network; supernetwork; travel behaviour; multiple user classes; time constraints.

1. INTRODUCTION

Travel behaviour analysis has been a hot topic in transportation research as it is regarded as the cornerstone for studying urban transportation network problems, which include travel demand forecasting, road pricing policy formulation and mitigating traffic congestion [1-4]. Among the majority of these traditional travel behaviour studies, the trip-based approach is mostly used [5-9]. In the trip-based approach, the network travel time is usually assumed to be dependent on the time-varying traffic velocity throughout a trip (i.e. an origin-destination pair) as well as the trip length and is evaluated by the integral of trip duration over each travel distance increment of user's trip. As a result, the origin, destination, departure time and transport mode of each trip are assumed to be identical to homogeneous users in the trip-based models. Therefore, the activity-based approach has arisen in recent decades to investigate users' daily multi-modal multi-activity trip chains, and there appeared a substantial body of literature using the activity-based approach to study users' travel choices [10-14]. In the activity-based approach, users' activity choices including activity sequence, activity type, activity location and time arrangement of each activity/trip are integrated into their travel choices (e.g. departure time, route and travel time) so that individuals' daily activity-travel patterns can be studied and explained in a more behaviourally realistic manner. Unlike the trip-based approach, the activity-based approach facilitates to conduct of a comprehensive study on the interactions among users' activity/travel choices, transportation network and activity location plan.

The introduction of the activity-based approach into transport models has motivated an emerging shift from focusing on single trips to comprehensively understanding transportation network users' daily activity-travel patterns. Within the framework of activity-based modelling, an individual user's activity schedule is explicitly investigated, in consideration of why an individual user's trip involves a specific activity, and when, where, with whom, by which transport mode, for how long and how frequently this activity is conducted [15]. Therefore, activity-travel scheduling has become a core component of many activity-based transport models. More specifically, the scheduling of a given set of selected activities consists of two steps: identifying feasible activity-travel agendas, and selecting the best activity-travel patterns under specific criteria. The concept of the time-space prism is usually used to assess the feasibility of planned activity-travel schedules [16], whereas optimisation models are employed in many studies to find the activity-travel schedule with a maximum utility or a minimum travel time [17-21].

Due to the complexity of linkages among various activities and travel, these mathematical analytical activity-based transport models rely heavily on the supernetwork representation where the basic transportation network is augmented with virtual (dummy) links to represent several travel choice dimensions such as time and space [22-31]. Such augmented networks are referred to as supernetworks. Among these studies, two supernetwork representation approaches have been widely used in recent years. One is the multi-state supernetwork approach, which was developed by Liao et al. [22] to examine user activity and travel behaviour. This approach was applied to different transport model settings with the consideration of user parking behaviour [23], space-time constraints [24] and land use scenarios [25]. Liu et al. [26, 27] adopted the enhanced supernetwork method to deal with dynamic activity-travel assignment problems. Another is the activity-time-space supernetwork approach, which is proposed by Ouyang et al. [28] to investigate the activity and travel scheduling problem within congested networks. Their approach was further developed to model related scheduling problems in multi-modal transit networks [29], and to address joint activity scheduling problems [30, 31]. However, a common drawback of these two approaches is that the resulting supernetwork may become very large, complex and even intractable when multiple spatial and temporal nodes and links are integrated into a single representation to capture the dynamics in activity-travel scheduling. Consequently, research efforts are required to be devoted to further developing more efficient supernetwork representation approaches in reducing network size and/or computational complexity.

Space and time constraints arose in the activity-travel scheduling problem under many conditions by which individual users' activity and travel decisions may be strongly affected [16, 24]. This is because activities such as sleeping at home, eating and going to work are usually conducted in regular rhythms and intervals. Public transportation service schedules also define potential limits on the execution of activities if such transport mode is optional. Finally, authority constraints on activity locations such as opening hours and service capacity constrain the time and place when and where individual users can choose to conduct a particular activity. In addition, transportation network users may be classified into different types where users in the same class have a similar valuation of travel time and thus homogeneous activity-travel behaviour [32-38]. The activity-travel behaviour of one class of users can be very different from that of another class of users. For example, compared with workers, non-workers such as retired individuals, homemakers and unemployed individuals often participate in more household-related activities including shopping, drop off/pick up, recreation, eating out, visiting and even staying at home for various household purposes. Furthermore, due to the flexibility in daily activity-travel scheduling, non-workers always choose to conduct out-of-home activities in off-peak periods and good weather, rather than suffering peak period congestion or bad weather. Such differences between workers' and non-workers' activity-travel behaviour may have a significant impact on the transportation system and transportation-related policies and planning. However, as pointed out by [39], non-workers' activity-travel behaviour has not been well understood and studied so mathematical analytical studies that incorporate the impact of travel behaviour differences among multiple classes of users on activity-travel scheduling are still needed to contribute to this research area.

Motivated by these observations, a dynamic activity-travel scheduling problem is addressed in this paper where the impact of activities, the total time constraint and the distinct performance of multiple user classes are comprehensively considered. A supernetwork representation approach is introduced to generate the activity-journey network which expands the basic transportation network in both time and space dimensions. With the supernetwork representation, an activity-based network user equilibrium model is formulated and transformed into a static network flow assignment problem. A solution algorithm is then developed to find the path with the maximum utility in the AJN from the start node to the end node for each user. A numerical study is conducted to illustrate the application of the proposed model and solution algorithm for real-world transportation networks. Compared with existing literature, the main contribution of this paper lies in: (1) jointly considering the activity-travel scheduling problem with time constraints and multiple user classes; and (2) developing a supernetwork representation approach with lower network complexity and demonstrating its potential applicability to large-scale transportation networks.

The remainder of this paper is organised as follows. In the Methodology section, a supernetwork, namely, the activity-journey network is presented in Section 2.1. An illustration of AJN is provided in Section 2.2 to show the details of the representation of activity and travel choices by activity links and journey links in the AJN. The link utility, link time and link capacity of the AJN are discussed in Section 2.3. The choice results of multi-class users' activities and travels are depicted by link utilities and link times. In Section 2.4, an activity-based network user equilibrium model is formulated to deal with the resulting network flow assignment problem under time constraints. A solution algorithm is proposed in Section 2.5. Based on the application of the proposed model and solution algorithm in several transportation networks, numerical results are analysed and discussed in a combined Results and discussion section, Section 3. Finally, we conclude the paper in Section 4.

2. METHODOLOGY

This section details the formulations of the dynamic activity-travel scheduling problem and the solution algorithm. An activity-journey network representation of the basic transportation network is first introduced, where the basic transportation network is expanded by augmented nodes and links to represent various travel choice dimensions such as when to take a trip, by which route, to what destination and for what activity. The link utility, link time and link capacity of the AJN are discussed. Then the dynamic activity-travel scheduling problem can be modelled as a user equilibrium model with variable travel demand, trip distribution and traffic assignment components using the proposed supernetwork representation. Based on the explicit modelling of link interactions in terms of time and space, a solution algorithm is developed to find the user equilibrium flow pattern over the supernetwork.

2.1 The generation of an activity-journey network

Denote the basic transportation network as $\bar{G} = (\bar{B}, \bar{A})$, where $\bar{B}$ is the set of nodes and $\bar{A}$ is the set of travelling links in $\bar{G}$. Assume that some nodes in $\bar{B}$ are activity location nodes where users could conduct activities. Here, activity location nodes are functional zones (represented by the geometrical centre of gravity) in urban areas where certain activities are performed, such as residential districts, central business districts, restaurant districts and shopping plazas, etc. A single activity is denoted as j, whereas a single activity location node is denoted as d. Let D and J denote the set of all activity location nodes and all activities in $\bar{G}$, respectively. Let J_d be the set of activities which could be engaged in by users at node d. Then we have $j \in J$, $d \in D$, $J_d \subseteq J$, and $D \subseteq \bar{B}$.

Here, an activity-journey network approach is introduced to generate an expanded supernetwork based on $\bar{G}$. The main idea of the AJN expansion is to illustrate the activity choices and journey choices of travelling from one activity location to the subsequent activity location, along the time and space dimension within the basic transportation network.

Let $G = (B, A)$ denote the generated AJN, where B is the set of nodes in AJN and A is the set of links in AJN. The total schedule time T is assumed to be identically divided into $\bar{K}$ intervals where the length of a time interval is T_L. Users could make their activity choices or travel choices at the start time of each time interval k, where $k = 1,2,\dots,\bar{K}$. Note that $\bar{K}+1$ is the end time of the last time interval $\bar{K}$. The procedures of generating the AJN are listed below.

Step 1. Enumerate all feasible activity and activity location combinations (j, d) in the basic transportation network for all $j \in J_d$ and $d \in D$. For a single activity location node d, there exists at least one such combinations since J_d is a non-empty set.

Step 2. For each combination (j, d) in the basic transportation network $\bar{G}$, construct $\bar{K}+1$ nodes in the AJN, and each node is denoted as $b_k^{j,d}$, where $d \in D$, $j \in J_d$, $k = 1,2,\dots,\bar{K}+1$.

Step 3. For each node $b_k^{j,d}$, construct a link for each time interval k (where $k = 1,2,\dots,\bar{K}$) from node $b_k^{j,d}$ to node $b_{k+1}^{j,d}$ in the AJN, which is denoted as link $(b_k^{j,d}, b_{k+1}^{j,d})$.

Step 4. For each node $b_k^{j,d}$, construct a link from node $b_k^{j,d}$ to node $b_{k'}^{j',d'}$ in the AJN, which is denoted as link $(b_k^{j,d}, b_{k'}^{j',d'})$, where $d, d' \in D$, $j \in J_d$, $j' \in J_{d'}$, $k, k' \in \{1,2,\dots,\bar{K}+1\}$, $k' = k + \Gamma_{d,d'}(k)$, and $\Gamma_{d,d'}(k) = \lceil \Gamma'_{d,d'}(k)/T_L \rceil$.

Here, k is the departure time from activity location d after conducting activity j, k' is the start time of participating in activity j' at activity location d', $\Gamma'_{d,d'}(k)$ is the minimum travel time (i.e. the user equilibrium time) from d to d' when the departure time is k, and $\Gamma_{d,d'}(k)$ is the rounded-up integer multiple of T_L for $\Gamma'_{d,d'}(k)$.

Step 5. Introduce a dummy start node S and a dummy end node E to the AJN.

Step 6. Construct a start link $(S, b_1^{j,d})$ from node S to node $b_1^{j,d}$ (where 1 is the start time of the time horizon) and an end link $(b_{\bar{K}+1}^{j,d}, E)$ from node $b_{\bar{K}+1}^{j,d}$ (where $\bar{K}+1$ is the end time of the time horizon) to node E for each combination (j,d) where $j \in J_d$ and $d \in D$.

The relationship between the nodes and links in the basic transportation network $\bar{G}$ and AJN are as follows. For an activity location node $d(d \in D)$ in the basic transportation network which can perform N_d ($N_d = |J_d|$) activities, it generates N_d initial nodes corresponding to the number of activities, and then each node is further augmented into $\bar{K}+1$ nodes along the time dimension. Since the node in AJN is characterised by activity location, activity type and start time, there are activity links and journey links in AJN. Activity links are generated in Step 3 which represent the time duration of an activity within the same activity location, whereas journey links are generated in Step 4 which represent the movements between different activity locations. In addition, two dummy nodes S and E are employed in AJN in Step 5, then start links and end links are generated. Compared to the basic transportation network $\bar{G}$, only the journey links (of the four types of links) in AJN are similar (but not the same) to the links in $\bar{G}$.

In general, the set of nodes in AJN, B contains all the nodes $b_k^{j,d}$ generated in Step 2, and two dummy nodes S and E. Assume that the number of combinations (j,d) for all j and d in the basic transportation network $\bar{G}$ is X_1. Then it is easy to see that the number of nodes in AJN is $X_1 \times (\bar{K}+1) + 2$. For a given combination (j,d), there are $\bar{K}$ activity links among $\bar{K}+1$ nodes, one start link from start node S to node $b_1^{j,d}$, and one end link from node $b_{\bar{K}+1}^{j,d}$ to end node E. Therefore, the number of activity links, start links and end links in AJN are $X_1 \times \bar{K}$, X_1 and X_1, respectively. The estimation of the number of journey links is as follows. To make sure the journey from location d to location d' is feasible, $\Gamma_{d,d'}(k)$ must satisfy that $k' = k + \Gamma_{d,d'}(k) \le \bar{K}+1$, i.e. users should arrive at activity location d' within the schedule time horizon. For a given combination (j,d), the number of potential journey links to activity location d', $N_{d,d'}$ is the number of the feasible set of departure time k from activity location d, where $0 \le N_{d,d'} = \lfloor \bar{K}+1-\Gamma_{d,d'}(k) \rfloor \le \bar{K}+1$. Thus, the number of journey links in AJN can be expressed as $\sum_{d \neq d',\, d,d' \in D} N_{d,d'}$, which is the sum of the number of the feasible set of departure time for all possible journeys. Then the total number of links in AJN is the sum of the number of these four types of links, that is, $X_1 \times (\bar{K}+2) + \sum_{d \neq d',\, d,d' \in D} N_{d,d'}$. Recall that $\Gamma_{d,d'}(k)$ represents the travel time from location d at departure time k to location d' in the form of an integer multiple of time intervals. When $\Gamma_{d,d'}(k)$ is sufficiently large, there is no journey link between activity locations d and d', and thus $N_{d,d'}$ takes the minimum value. On the other hand, the maximum value of $N_{d,d'}$ is obtained when $\Gamma_{d,d'}(k)$ is 0, i.e., users may switch from activity j to activity j' within the same location node. Consider that for each combination (j,d) there are $X_1 - 1$ possible journeys to other activity and location combinations, the number of journey links is bounded by 0 and $X_1 \times (X_1 - 1) \times (\bar{K}+1)$. Therefore, the lower and upper bound on the number of links in AJN are $X_1 \times (\bar{K}+2)$ and $(X_1)^2 \times (\bar{K}+1) + X_1$, respectively.

2.2 An illustration of the activity-journey network

Figure 1 shows a simple transportation network consisting of 5 nodes and 16 directional links. Nodes are numbered from 1 to 5, and links are indexed from 1 to 16. Four activity location nodes represent four zones, namely, the home or residential area (labelled as "H") for doing home-based activities, the restaurant area (labelled as "R") for eating activities, the shopping area (labelled as "S") for shopping activity and workplace (labelled as "W") for working activity and/or eating activity. The marginal utility of eating at a restaurant is much higher than that of eating at the workplace for network users.

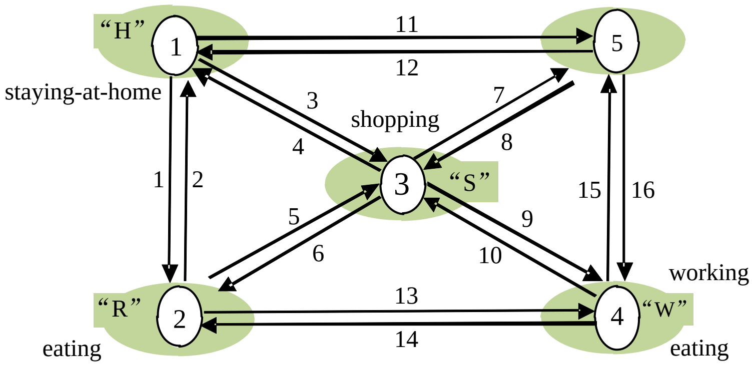

Figure 1 – An example of an urban transportation road network

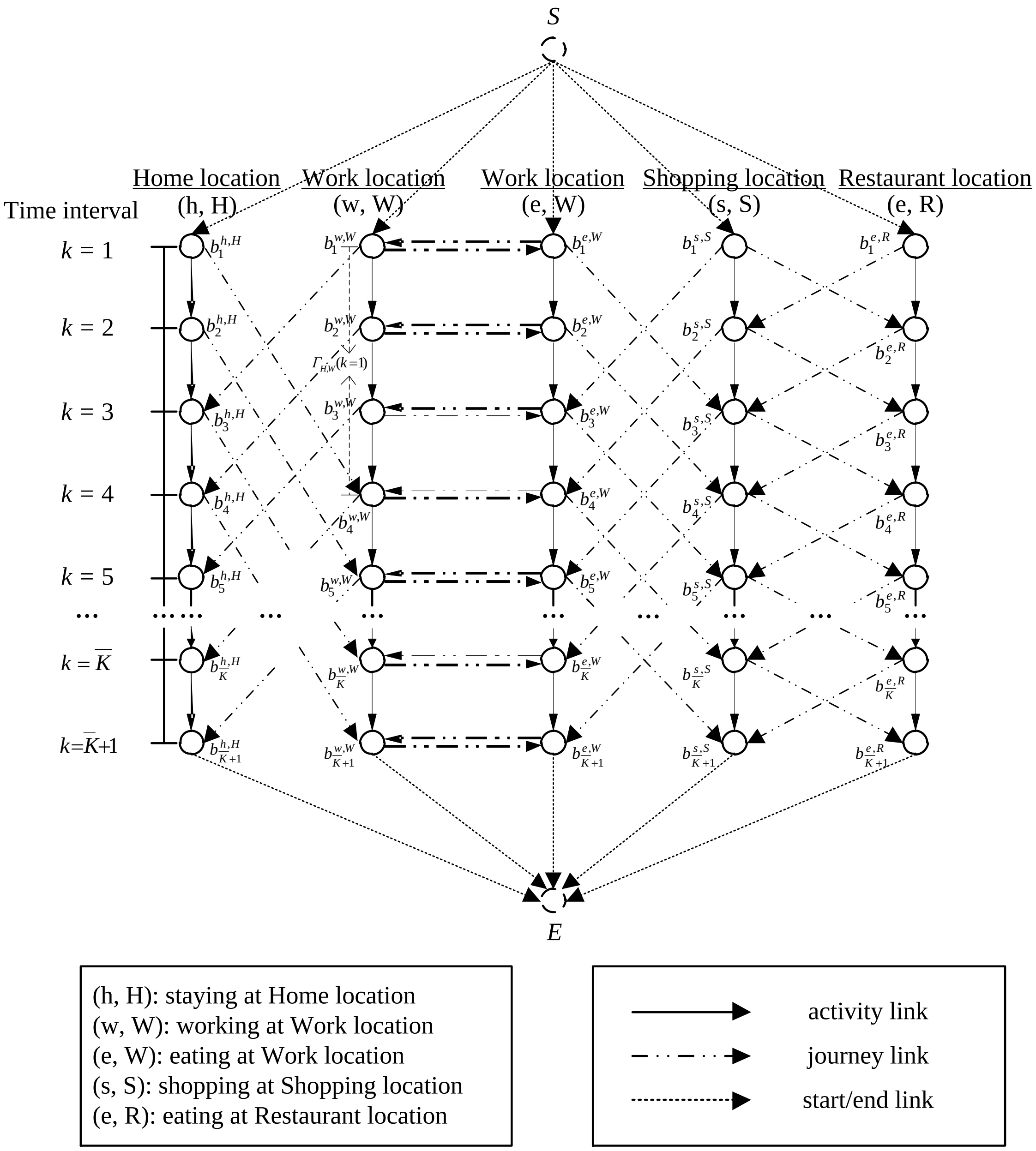

Figure 2 – The illustrated AJN of the urban transportation road network

The activity-journey network, which is an expansion of the basic transportation network in *Figure 1*, is illustrated in *Figure 2*. There are five combinations of activity and activity location node (i.e. $X_1 = 5$): (h, H), (w, W), (e, W), (s, S) and (e, R), where the staying-at-home activity, working activity, eating activity and shopping activity are denoted as "h", "w", "e" and "s", respectively. For example, combination (e, R) represents conducting "eating" activity at location node "Restaurant". Each combination is augmented into $\bar{K}+1$ nodes along the time dimension. Activity links are generated by the time duration of conducting an activity within the same activity location (i.e. the vertical links between nodes in AJN). For example, it will take several time intervals for users to stay at home or work in the workplace. Journey links are generated by the possible movements between different activity locations, which depend on the related travel time. In general, it will take several time intervals for users to travel (and switch) from one activity location (and one type of activity) to another. However, if users are performing different activities within the same location (i.e. the horizontal links between nodes in AJN), the travel time is assumed to be 0. Since there are 20 (i.e. $X_1 \times (X_1 - 1) = 5 \times 4$) possible journeys between different activity and activity location combinations, and the detailed journey links are further determined by the travel time between different activity locations, *Figure 2* just displays some of the possible journey links. More specifically, the travel time from the home node to the workplace node with departure time $k = 1$, $\Gamma_{H,W}(k=1)$ is set to be 3-time intervals in the illustration. Finally, start links and end links are generated to show how users enter and exit the AJN.

2.3 Link utility, link time and link capacity

For simplicity of description, use A^J, A^T, A^O and A^D to represent the set of activity links, journey links, start links and end links in the AJN, respectively. It is assumed that users can be classified into different types according to their evaluation of time (i.e. link utility). Specifically, let v_a^m denote the link utility of link a for users in class m. In contrast, the link time of link a in the AJN, t_a is assumed to be identical for all users. The determination of v_a^m and t_a in the AJN are summarised as follows.

Case I. If $a \in A^O$, or $a \in A^D$, then link a represents the virtual process of entering or exiting the AJN through the dummy node S or E. Thus, for any user in any class m, the link utility and link time of link a are both 0, i.e., $v_a^m = 0$, and $t_a = 0$.

Case II. If $a \in A^J$, then link a is an activity link, and users obtain activity utility from engaging in an activity j at location d for the one-time interval with start time k, which can be expressed as $v_a^m = \int_k^{k+1} u_{j,d}^m(\omega)d\omega$, where $u_{j,d}^m(\omega)$ is the marginal utility of conducting activity j at location d at time ω for users in class m, and depends on the node flow and the accommodating capacity of location d in $\bar{G}$. Here, the node flow of location d is defined as the total number of users engaging in activity j at location d at time interval k. In this case, the link time of link a is 1 time interval for all types of users, i.e. $t_a = 1$.

Case III. If $a \in A^T$, then link a is a journey link, and users suffer travel disutility from spending travel time $\Gamma_{d,d'}(k)$ to move from location d with departure time k to location d', which is $v_a^m = -\sigma_m \Gamma_{d,d'}(k)$, where σ_m is the marginal utility per time interval for users in class m. In this case, the link time of link a is $\Gamma_{d,d'}(k)$ time intervals for all types of users, i.e., $t_a = \Gamma_{d,d'}(k)$.

Let C_a represent the capacity of link a (in terms of the number of users) in the AJN. The determination of C_a is given as follows.

Case I. If $a \in A^O$, or $a \in A^D$, then $C_a = \infty$, i.e., there are no capacity constraints on the start and end links.

Case II. If $a \in A^J$, then the capacity of an activity link is $C_a = Q_{j,d}(k)$, where $Q_{j,d}(k)$ is the capacity of activity location d for users conducting activity j at time interval k.

Case III. If $a \in A^T$, then the capacity of a journey link is $C_a = \min_{h \in P_{d,d'}(k)} Q_h$, where h is a single link of the basic transportation network $\bar{G}$, Q_h is the capacity of link h, and $P_{d,d'}(k)$ is the set of links experienced by the journey of travelling from origin d to destination d' with departure time k in $\bar{G}$. This implies that the capacity of a journey link in AJN (which may be a route in $\bar{G}$) is restricted to the capacity of the bottleneck link on the route of the journey in $\bar{G}$.

2.4 Model formulation

Without loss of generality, it is usually assumed that users in each class are pursuing the maximum utility when determining the decisions of travel choices and activity choices. Consequently, in the basic transportation network $\bar{G}$, users in each class must optimise their activities and travel plans under time constraints on the scheduled time horizon (for example, within a whole day) to achieve maximum utility. By introducing the expanded activity-journey network, this optimisation problem is transformed into a problem of identifying the path with the maximum utility in the AJN from node S to node E for each user. Furthermore, user equilibrium is globally achieved when *individual user cannot improve their utility by unilaterally altering their activity choice or travel choice to any other feasible options under the total time constraint*.

The list of variables and parameters used in model formulation is summarised as follows;

x_a	link flow (i.e. the number of users) on link a in the AJN, decision variable
$\boldsymbol{x}$	vector of x_a
x_a^m	the flow of users in class m selecting link a
r	a single route from node S to node E
q^m	total number of users in class m
q_r^m	the flow of users in class m selecting route r
$\delta_{a,r}$	a binary variable, 1 if link a is experienced by route r, and 0 otherwise.

The multi-class user equilibrium model is formulated as follows.

$$\max_{\boldsymbol{x}} Z(\boldsymbol{x}) = \sum_m \sum_a \int_0^{x_a} v_a^m(x)dx \tag{1}$$

subject to

$$q^m = \sum\nolimits_r q_r^m \quad \forall m \tag{2a}$$

$$x_a = \sum\nolimits_m x_a^m \quad \forall a \tag{2b}$$

$$x_a^m = \sum\nolimits_r \delta_{a,r} q_r^m \quad \forall a, m \tag{2c}$$

$$\sum\nolimits_a \delta_{a,r} t_a \le \bar{K} T_L \quad \forall r \tag{2d}$$

$$q_r^m \ge 0 \quad \forall r, m \tag{2e}$$

$$\delta_{a,r} \in \{0,1\} \quad \forall a, r \tag{2f}$$

Equation 1 is the objective function with the maximisation of the sum of link utility for all links and all users in the AJN, where v_a^m is defined in Section 2.3 for different type of links and depends on the size of link flow. In *Equation 2a*, the total number of users in each class is decomposed to the sum of the number of users in that class selecting all the routes. Similarly, in *Equation 2b* the link flow on a link is decomposed to the sum of the number of users in all classes selecting that link. More specifically, in *Equation 2c* the number of users in any class selecting a link is calculated by the sum of number of users in that class selecting all the routes that contain the link. *Equation 2d* implies that the sum of all link times on any route should be no larger than the length of the schedule time horizon. *Constraints 2e and 2f* are standard non-negativity and binary restrictions on the variables, respectively.

Although link capacity C_a is discussed in Section 2.3, capacity constraints such as $x_a \le C_a$, $\forall a$ will not be introduced directly to the above-mentioned model. The main reason is that the well-known BPR (bureau-public-road) function is employed in this study to characterise the mathematical relationship between link flow, link time and link capacity, which allows us to deal with the cases that link flow exceeds link capacity (realistic cases that can be seen in road transportation network with traffic jams). Furthermore, when such extreme cases are observed in the AJN it is also assumed that there is a rapid decline in link utility. More specifically, when link flow x_a is beyond link capacity C_a, there will be a significant reduction in marginal utility $u_{j,d}^m(\omega)$ for all the activity links (i.e., $a \in A^J$), or a considerable increase in the link time $\Gamma_{d,d'}(k)$ for all the journey links (i.e. $a \in A^T$).

2.5 Solution algorithm

In this section, we develop a solution algorithm for solving the utility maximisation problem presented in Section 2.4. Since the link utility function $v_a^m(x)$ is not convex in link flow x, the convexity of $Z(\boldsymbol{x})$ in *Equation*

1 with respect to x_a $(\forall a)$ cannot be guaranteed. However, note that $Z(\boldsymbol{x})$ is continuous and bounded in x_a $(\forall a)$, there exists at least one extreme point that maximises $Z(\boldsymbol{x})$. Based on the line-search method, the optimal solution can be obtained by iteration.

In general, the solution algorithm relies on the supernetwork representation and the all-or-nothing assignment method. Under the activity-based modelling approach, the dynamic activity-journey scheduling problem on the basic transportation network is transformed into a static traffic assignment problem on the expanded activity-journey network (i.e. a supernetwork), where the user equilibrium (UE) flow pattern is the result of each rational user from all classes taking the path with the maximum utility in the AJN from start node to end node. Accordingly, the network loading mechanism used in the algorithm designed to solve the UE problem assigns each origin-destination (i.e. from start node to end node) flow to the maximum-utility path connecting this O-D pair for specific link travel times. This traffic assignment procedure is known as the "all-or-nothing" assignment. Since the link travel time is state-dependent which is determined by the link flow for any link a, the proposed solution method involves a repetitive all-or-nothing assignment in which the link flows (as well as link travel times) resulting from the previous assignment are used in the current iteration. More specifically, the initial activity-journey-network is generated under the case where link flows in the basic transportation network are set to be 0 (and then the journey time between any two location nodes equals the free-flow travel time). The initial solution is obtained by the all-or-nothing assignment approach, i.e. assign all the users to a feasible route, and calculate the initial link flows in the AJN, as well as the node flows and link flows in the basic transportation network. In each iteration, new journey times are calculated since the link flows in the basic transportation network are updated. Then a new AJN with new journey links is generated since journey times are updated. The link flows in the new AJN are obtained by the line-search method, where the search direction is determined by the all-or-nothing assignment approach. Such processes are repeated until the stopping criteria are satisfied.

The detailed procedure of the solution algorithm is outlined as follows.

Step 1. Initialisation.

(1.1) Set the iteration index as $n=1$. For ease of exposition, we put superscript (n) on some notations to represent the values in iteration when necessary.

(1.2) Generate the AJN based on the basic transportation network $\bar{G}$. The journey time $\Gamma_{d,d'}(k)$ in AJN is obtained by solving the conventional time-dependent or dynamic trip-based traffic user equilibrium problem in $\bar{G}$, where the link flow of link h in $\bar{G}$ at time interval k, $f_h(k)$ is set to be 0.

Note that $f_h(k)$ is the link flow of link h (which is a physical road link) in the transportation network $\bar{G}$ at time interval k, whereas x_a is the link flow on link a (which may be a route in $\bar{G}$ consisting of several physical road links) in the AJN.

(1.3) Find a feasible route r from node S to node E in AJN, serving as an initial solution to the utility maximisation problem, i.e. all the users select the same route r.

(1.4) Assign all flows of a user class m to route r (i.e., let $q_r^m = q^m$), then the initial link flow $x_a^{m,(1)}$ of user class m in the AJN is calculated by $x_a^{m,(1)} = \delta_{a,r} q_r^m = \delta_{a,r} q^m$, where the value of $\delta_{a,r}$ is obtained from investigating whether link a is on route r.

(1.5) The link flow $x_a^{(1)}$ is calculated by the summation of link flows $x_a^{m,(1)}$ of all user classes, where $x_a^{(1)} = \sum_m x_a^{m,(1)}$, $\forall a$.

(1.6) Using link flow $x_a^{(1)}$ of the AJN, calculate the flow of activity location node d at time interval k for users in class m (denoted as $q_{j,d}^{m,(1)}(k)$), and the flow of link h at time interval k for users in class m (denoted as $f_h^{m,(1)}(k)$) in $\bar{G}$.

Step 2. Generation of new AJN and calculation of node flows and link flows in $\bar{\boldsymbol{G}}$ for iteration $\boldsymbol{n}$ $(\boldsymbol{n} \geq \boldsymbol{2})$.

(2.1) Calculate the journey times $\Gamma_{d,d'}^{(n)}(k)$, and the marginal activity utility of users in class m, $u_{j,d}^{m,(n)}(k)$ according to node flows $q_{j,d}^{m,(n-1)}(k)$ and link flows $f_h^{m,(n-1)}(k)$.

(2.2) Generate a new AJN with new journey links since journey times $\Gamma_{d,d'}^{(n)}(k)$ are updated.

(2.3) Update link utility v_a^m, link time t_a, and link capacity C_a of link a $(\forall a)$ in the new AJN, based on $\Gamma_{d,d'}^{(n)}(k)$ and $u_{j,d}^{m,(n)}(k)$.

(2.4) Find the route $r^{(n)}$ with the maximum utility from node S to node E in the new AJN.

(2.5) Assign all flows of a user class m to route $r^{(n)}$, where the new link flow $\bar{x}_a^{m,(n)}$ in AJN is $\bar{x}_a^{m,(n)} = \delta_{a,r^{(n)}} q^m$, where the value of $\delta_{a,r^{(n)}}$ is obtained from investigating whether link a is on route $r^{(n)}$.

(2.6) According to the line-search method, the new search direction for solving the utility maximisation problem is determined by $(\bar{x}_a^{m,(n)} - x_a^{m(n-1)})$, and the link flow $x_a^{m,(n)}$ of user class m in the new AJN is given by $x_a^{m(n)} = x_a^{m(n-1)} + \lambda\left(\bar{x}_a^{m,(n)} - x_a^{m(n-1)}\right)$, where λ is the search step size.

(2.7) Using link flow $x_a^{(n)}$ of the new AJN where $x_a^{(n)} = \sum_m x_a^{m,(n)}, \forall a$ to update activity location node flows $q_{j,d}^{m,(n)}(k)$ and link flows $f_h^{m,(n)}(k)$ in $\bar{G}$.

Step 3. Loop of convergence tests.

If the stopping criteria are satisfied simultaneously, then terminate the iteration and output the solution. Otherwise, set the iteration index as $n = n + 1$, and go to Step 2.

Here, we introduce the following stopping criteria, where the gaps of link flow x_a^m in the AJN, the activity location node flow $q_{j,d}^m(k)$ and the link flow $f_h^m(k)$ in $\bar{G}$ between two consecutive iterations should be lower than the pre-determined errors ε_1, ε_2, and ε_3, respectively.

$$\sqrt{\sum_m \sum_a (x_a^{m,(n+1)} - x_a^{m,(n)})^2} \Big/ \sum_m \sum_a x_a^{m,(n)} \le \varepsilon_1 \tag{3}$$

$$\sqrt{\sum_m \sum_h \sum_k \left(f_h^{m,(n+1)}(k) - f_h^{m,(n)}(k)\right)^2} \Big/ \sum_m \sum_h \sum_k f_h^{m,(n)}(k) \le \varepsilon_2 \tag{4}$$

$$\sqrt{\sum_m \sum_{d\in D} \sum_{j\in J_d} \sum_k (q_{j,d}^{m,(n+1)}(k) - q_{j,d}^{m,(n)}(k))^2} \Big/ \sum_m \sum_{d\in D} \sum_{j\in J_d} \sum_k q_{j,d}^{m,(n)}(k) \le \varepsilon_3 \tag{5}$$

The flowchart of the solution algorithm is given in *Figure 3*.

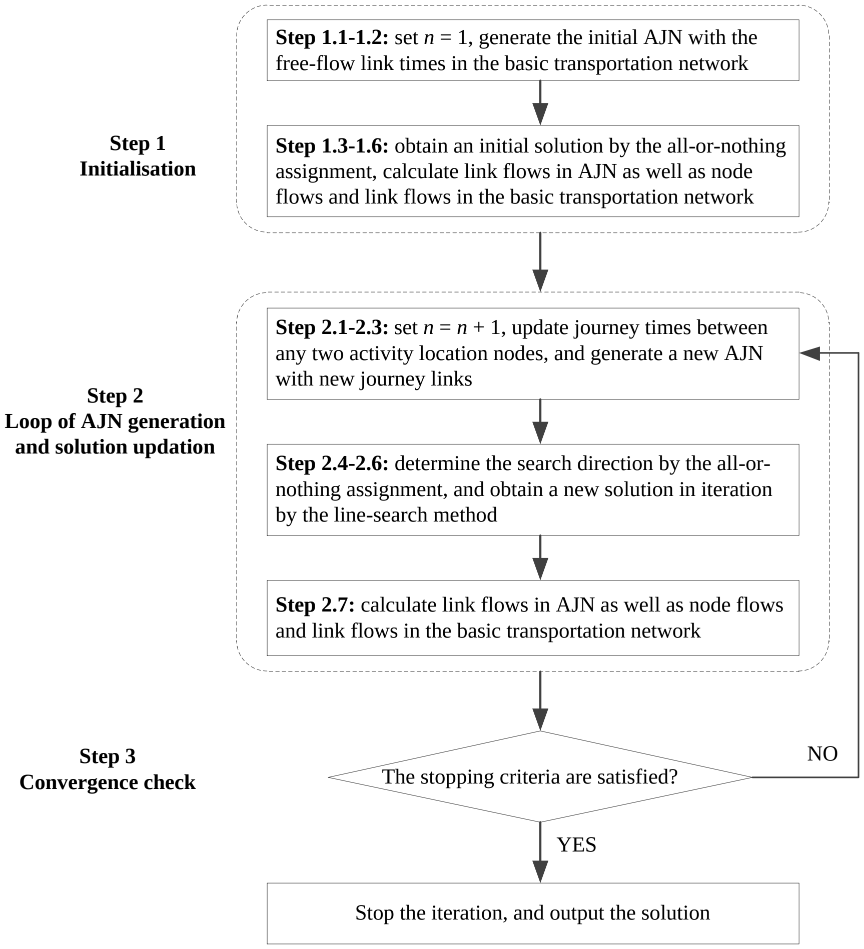

Figure 3 – The flowchart of the solution algorithm

3. RESULTS AND DISCUSSION

3.1 A small network

The transportation network studied in the first numerical example is illustrated in *Figure 1*, which has 16 directional links and 5 nodes. The time-dependent travel time $t_h(k)$on road link h at time interval k in the basic transportation network, could be given by the following bureau-public-road (BPR)-type link travel time function of *Equation 6*, where the required parameters are specified in *Table 1*

$$t_h(k) = t_h^0\left(1.0 + 0.15\left(\frac{f_h(k)}{Q_h}\right)^4\right), h \in B \tag{6}$$

where t_h^0 is the free-flow link time of road link h.

Table 1 – Link free-flow travel time and capacity for the transportation road network

Link	1/2	3/4	5/6	7/8	9/10	11/12	13/14	15/16
Free-flow travel time t_h^0 (min)	20	20	20	20	20	10	20	20
Link capacity Q_h (vehicles/hour)	1800	1800	1800	1800	1800	1800	1800	1800

The population in the basic transportation network is composed of two user classes: workers where $q^1 = 3000$ and non-workers where $q^2 = 1500$. Workers will engage in all activities including work activity, whereas non-workers just perform non-work activities. The total schedule time horizon is a whole weekday, i.e. $[0{:}00, 24{:}00]$, which is equally divided into 144 discrete time intervals, that is, $T = 24$ hours, $\bar{K} = 144$, and $T_L = 10$ minutes. The marginal time utility for users in each class are $\sigma_1 = 30$ CNY/hour for workers and $\sigma_2 = 18$ CNY/hour for non-workers, where CNY is the abbreviation for Chinese yuan.

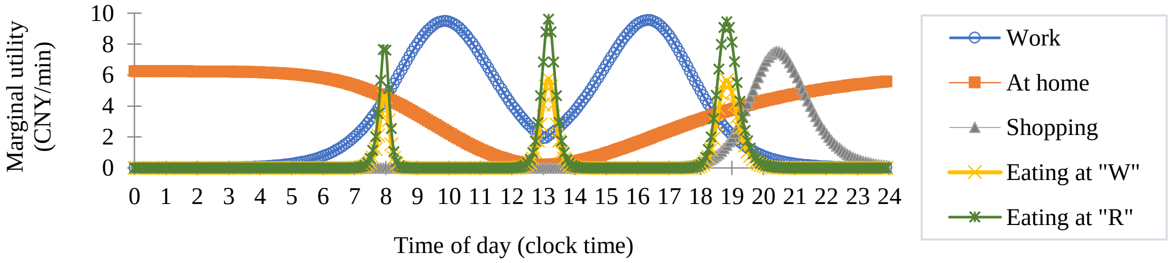

Figure 4 – Simplified marginal utility profiles of various activities

The marginal utility functions of activity engagement of workers, $u_{j,d}^1(k)$ are identical to those depicted in *Figure 4*. The marginal utility profiles of these activities are derived from the discussions on marginal utility functions of activity participation in the study of Ettema and Timmermans (2003) [40], which have been extensively adopted in various studies, as referenced in the literature [27-31]. The marginal utility of activities for non-workers is assumed to be 0.6 times those given in *Figure 4*, with the exception that the marginal utility of shopping activity is 1.5 CNY/minute from 9:00 to 22:00, and 0 during the remaining time of the whole day. The parameters for the convergence check of the solution algorithm are set as ε_1=0.001, ε_2=0.001, and ε_3=0.001, respectively.

The proposed solution algorithm was coded in MATLAB R2024b and run on a Windows PC with a 12th Gen Intel(R) Core (TM) i5-12500 CPU (3 GHz) and 8 GB RAM. The running time is 2635.73 seconds in total and 2.08 seconds on average for each iteration for each user group in this numerical example. The results of solving the multi-class travel behaviour problem in the exampled transportation network are as follows: 280 different activity and travel patterns (ATPs) are endogenously generated for 3,000 workers, and 120 different ATPs are endogenously generated for 1,500 non-workers. The typical ATPs taken by the highest number of workers (on the left half) and non-workers (on the right half) are presented in *Figure 5*. These two typical ATPs show that the users' travel behaviours are quite different between workers and non-workers. In each weekday, most workers leave home early, go to work and eat work meals, then go off work and return home at the end of the day. The daily activity chain for these workers is H→W→E→W→E→H, and the associated travel chain (in terms of physical links and nodes in $\bar{G}$) is node 1(H) → node 5 → node 4(W) → node 5 → node 1(H). However, most non-workers leave home late, go shopping and eat at a restaurant, and then return home after lunch. The daily activity chain for these non-workers is H→S→E→H, and the travel chain is node 1(H) → node 3(S) → node 2(R) → node 1(H).

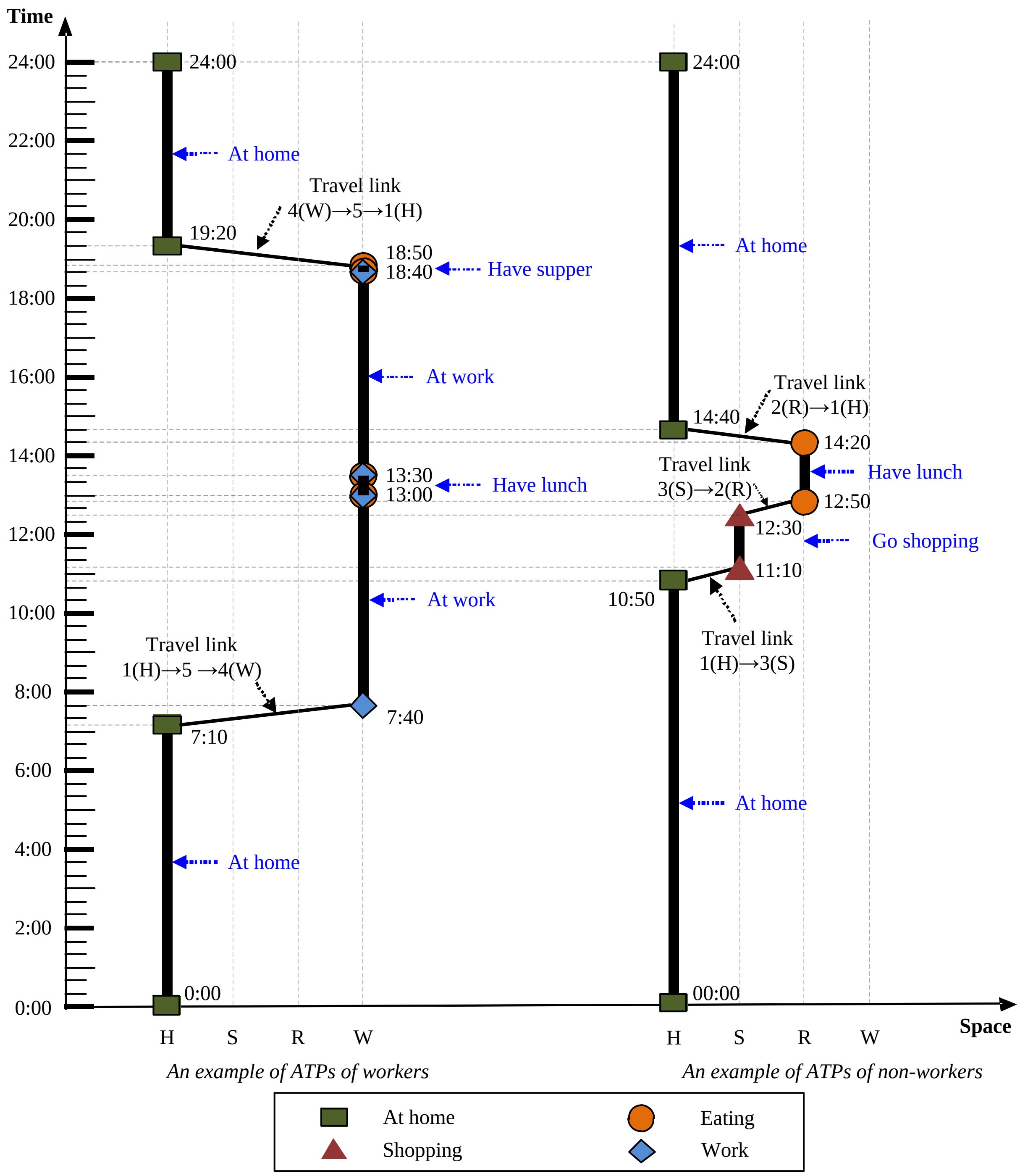

Figure 5 –The typical ATP most users selected in each class

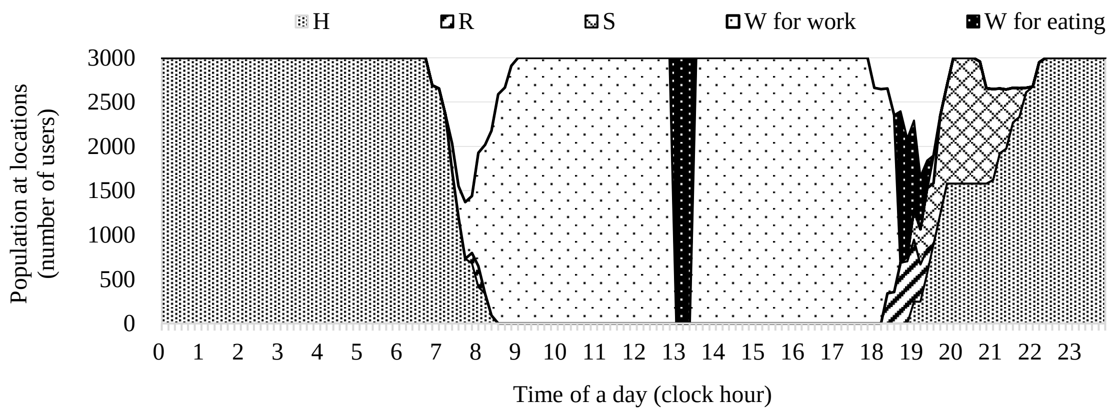

Figure 6 – Population distribution at activity locations of workers

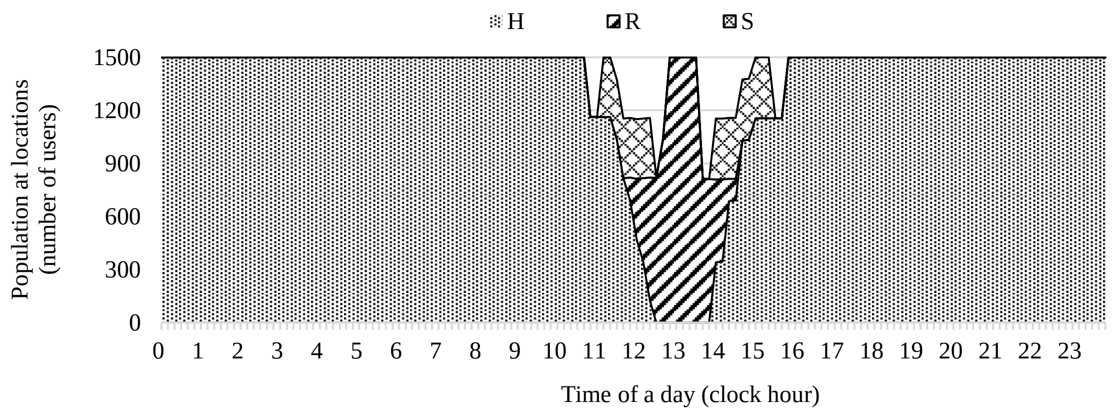

Figure 7 – Population distribution at activity locations of non-workers

Figure 6 and *Figure 7* depict the resulting population distributions at various activity location nodes for workers and nonworkers, respectively. Note that at any time interval during a day, a user is either at the location node or on a travel link from one location node to another. Thus, it can be seen that the population of workers (or non-workers) at activity location nodes is not always 3000 (or 1500), meanwhile, the rest of the workers (or non-workers) are on the travel links. The group travel behaviours of workers are as follows. In the morning, some workers leave home early, eat breakfast and then go to the workplace, while others eat breakfast at home, leave home late and go to work directly. In the middle of the day, they have lunch at the workplace. At the end of the day, some workers eat work meals at the workplace, some have dinner at the restaurant, while others return home and have supper at home. Shopping activity is usually scheduled in the evening after work activity and/or eating activity. In contrast, non-workers perform the shopping activity in the morning or afternoon, depending on their departure time from home. Since work activity is not a compulsory activity for them, they eat meals either at home or at a restaurant and return home much earlier than the workers.

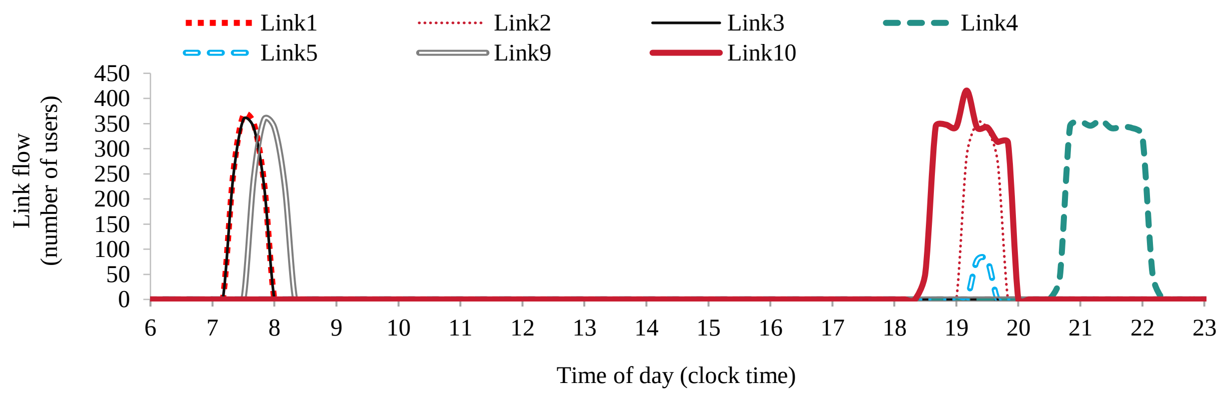

(a)

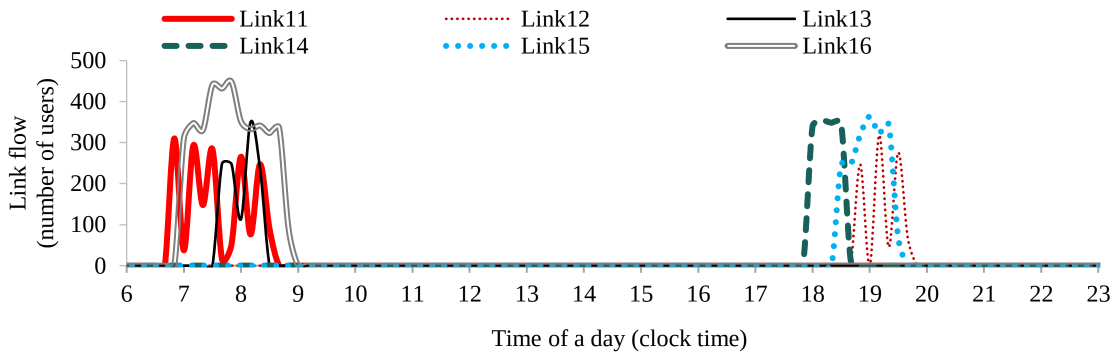

(b)

Figure 8 – Flow of workers along the time on links in the basic transportation network

Figure 8 and *Figure 9* present the resulting time-dependent link flows in the basic transportation network through the entire day for workers and non-workers, respectively. Compared with the population distribution at location nodes in *Figure 7*, it should be noted that only link flows in certain time intervals of a day are non-zeros.

It is shown in *Figure 8* that there exists a morning commute peak period for workers from 6:40 to 9:00 with the high traffic volumes on link 1, link 3, link 9, link 11, link 13 and link 16, and an afternoon commute peak period for workers from 17:50 to 20:00 with high traffic volumes on link 2, link 5, link 10, link 12, link 14 and link 15. An additional peak period from 20:30 to 22:20 is also observed on link 4, mainly because during that time period a group of workers are going back home after shopping. Conversely, it can be seen from *Figure 9* that non-workers depart from home after 10:30, much later than workers in the morning, in order to miss the morning rush hours caused by workers' travels from home to workplace. Similarly, they also return home before 16:00 to avoid the afternoon commute peak period caused by workers' travels from workplace to home.

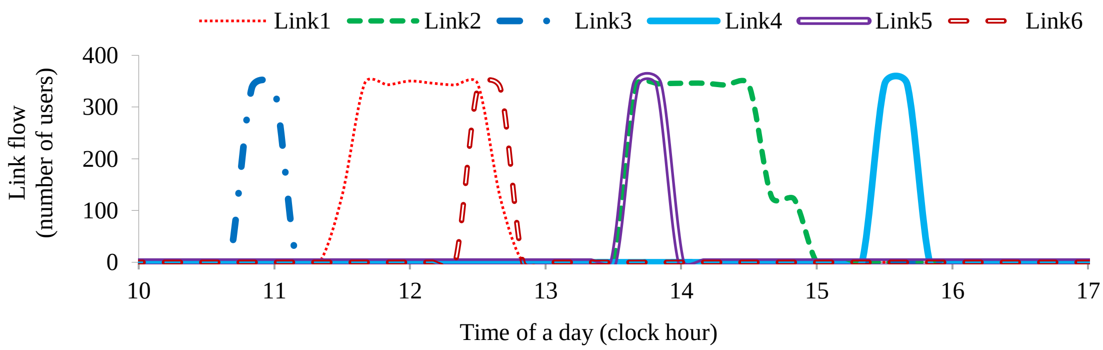

Figure 9 – Flow of non-workers along the time on links in the basic transportation network

3.2 Sioux Falls network and Anaheim network

The proposed model and solution algorithm are also applied to solve the activity-travel scheduling problems in the Sioux Falls network (medium-sized) and the Anaheim network (large-scale). With the same computer specifications and the same version of MATLAB software, the Sioux Falls network is solved in 1579.05 seconds, while the Anaheim network is solved in 2616.89 seconds. Rather than the simple transportation network in *Figure 1*, these large-scale real-world transportation networks are usually too complex to be graphically displayed, and the results are so complicated that it is difficult to explicitly illustrate and discuss users' travel behaviours for each ATP, node or link.

The Sioux Falls network includes 24 nodes and 76 links, which are numbered and shown in *Figure 10*. In this numerical example four types of activity location nodes are considered: home node (i.e. node 1 and 17), restaurant node (i.e. node 16) for eating, shopping node (i.e. node 10) and workplace (i.e. node 18). The capacity of each link between any two nodes is assumed to be 3600 users per hour. The free-flow link time is given for each numbered link in *Figure 10*. Two groups of workers with different home location nodes are considered: group 1 with a population of 3000 workers who live far away from downtown (i.e. node 1), and group 2 with a population of 3000 workers who live in the central business district (i.e. node 17). The time horizon of a whole weekday is equally divided into 144 time intervals, i.e. 10 minutes for one interval. The marginal time utility for users in each group is $\sigma = 18$ CNY/hour. Furthermore, the marginal utility functions of activity engagement for users are the same as shown in *Figure 3* except that the marginal utility of eating activity is 1.5 times higher than that in *Figure 3*. The parameters for the convergence check of the solution algorithm are given as ε_1=0.05, ε_2=0.05, and ε_3=0.05.

The results of solving the dynamic activity-travel scheduling problem defined in the Sioux Falls network are as follows: 92 different ATPs are generated for users in group 1, and 84 different ATPs are generated for users in group 2. Among these ATPs, the one which is adopted by the largest proportion (24%) of workers for each group includes the following activity chain: Home → Eating → Work → Eating → Work → Eating → Shopping → Home. The main difference in travel behaviour between the two groups of workers is that workers in group 1 leave home earlier but return home much later than workers in group 2.

Figure 11 depicts the resulting population distributions at various activity location nodes for workers in groups 1 and 2, respectively. It is clear in *Figure 11a* that there exists a gap in the population shift between the home node and workplace, which represents a relatively long-distance travel time between the two location nodes. Another gap between the shopping node and home node can be also observed in *Figure 11a* for workers in group 1 due to the similar time lag in the movement between the two nodes. Thus, such gaps are not so sharp in *Figure 11b* for workers in group 2. Moreover, since workers in groups 1 and 2 share the same workplace, eating node and shopping node, there are almost no difference in the population shift between these location nodes.

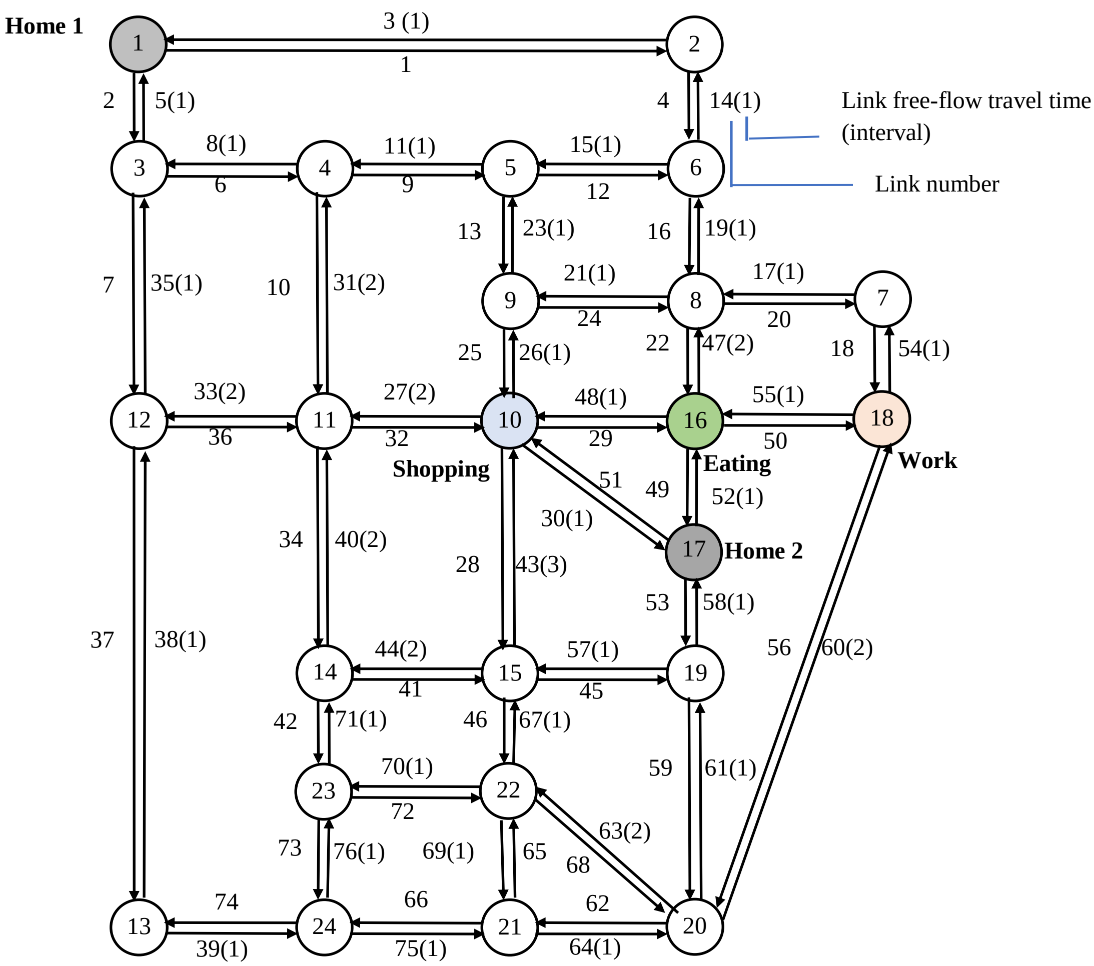

Figure 10 – Sioux Falls network

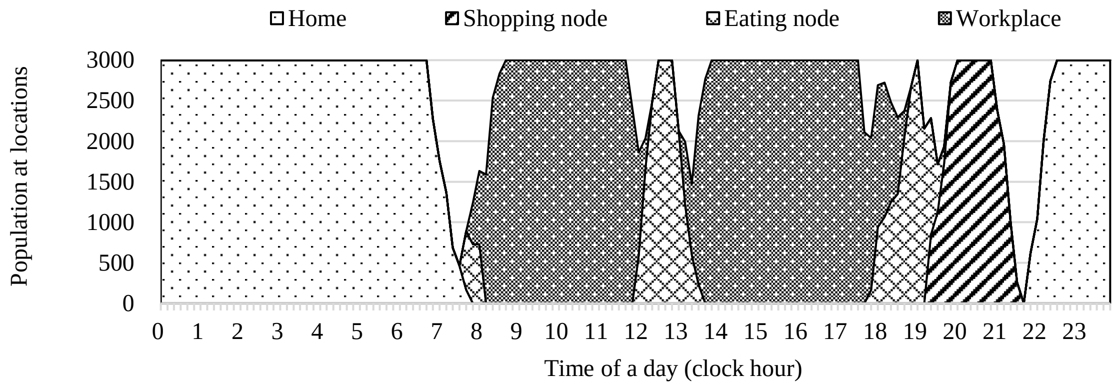

(a) users in group 1

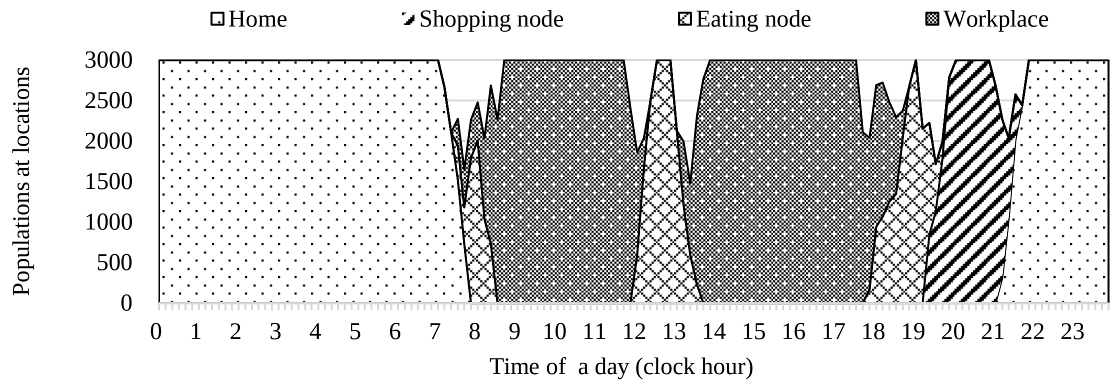

(b) users in group 2

Figure 11 – Population distribution at activity locations for workers in group 1 and group 2

The morning commute peak period for workers in group 1 is from 6:50 to 8:40 on the path of link 1, link 4, link 16, link 20, link 18 and link 22, while the night commute peak period is from 21:00 to 22:30 on the path of link 26, link 24, link 19, link 14, link 3, link 23, link 11, link 8 and link 5. The morning rush hour for workers in group 2 is from 7:20 to 8:00 on link 52, and the night rush hour is from 21:00 to 21:50 on link 30. Workers in group 2 suffer short commute peak periods and less disutility from the journeys in the transportation network, which illustrates the benefit of a jobs-housing balance. In addition, the joint travels of performing eating and/or shopping activities are observed on link 55, link 50 and link 48 for all the network users.

The Anaheim network consists of 416 nodes and 914 links. Detailed information on its road links and nodes can be found in [41]. Similar to the Sioux Falls network, four types of activity location nodes are considered: home node (i.e. node 200 and 272), restaurant node (i.e. node 269) for eating, shopping node (i.e. node 267) and workplace (i.e. node 266). Two groups of workers with distinct home locations are considered with the same population of 3000. The study time span is from 16:00 to 22:00 which is equally separated into 360 discrete time intervals, i.e. 1 minute for one interval. The marginal time utility for users in each group is $\sigma = 30$ CNY/hour. In addition, marginal utility functions of activity engagement for users are also given in *Figure 3*. The parameters for the convergence check of the solution algorithm are given as ε_1=0.05, ε_2=0.05, and ε_3=0.05. Numerical results of solving the dynamic activity-travel scheduling problem defined in the Anaheim network show that users work in the workplace until 18:30, then go to the restaurant node for dinner time from 18:35 to 19:35, go shopping after dinner, then return home after 21:20.

3.3 Discussion

In general, the application of the proposed model and solution algorithm to several transportation networks shows that network users' travel behaviour is well characterised and studied. The daily activity and travel patterns including activity choices and travel choices are derived for network users with the corresponding adoption rate, in which activity location, activity start time and duration, journey origination, departure time and route links are explicitly specified. The population shift between different location nodes across a day is illustrated to show the group travel behaviour of users, i.e. the main time period of performing certain activities, the sequence of activities, and the diversification of users' travel plans. The congested links as well as peak periods are also identified, which facilitates to better understanding of network traffic evolution and makes transport and urban land use policies more properly.

Moreover, the AJN approach proposed in this paper can be adapted to deal with multi-modal transportation networks by dividing the basic transportation network into a number of subnetworks with respect to the transit mode and expanding them to the activity journey network. The queuing behaviour in transportation networks can be investigated by the AJN approach by incorporating queuing links into the expanded activity-journey network. Similarly, parking behaviour can also be studied by allowing necessary cycle routes of flows in the activity-journey-network, i.e. users must return to the original parking node to pick up their car and then continue their journey in the transportation network.

Finally, a comparative analysis of the complexity of supernetwork representation is conducted among the AJN approach and two widely used approaches: the multi-state supernetwork approach [22] and the activity-time supernetwork (ATS) approach [28]. The former is proposed to deal with parking behaviour and multi-modal choice problems, whereas the latter is developed to investigate queuing behaviour in transportation networks. As mentioned above, the AJN approach can incorporate these considerations, but as shown below, requires a simpler supernetwork representation.

Table 2 – Sizes of the expanded multi-state supernetwork, ATS and AJN

	Multi-state supernetwork	ATS	AJN
Number of nodes	$2^{X_J}M(X_R+1)X_N$	$X_N(\bar{K}+1)+2+X_L(\bar{K}+1-0.5X_W)(X_W+1)-(X_W+1)\sum_h t_h^0$	$X_1(\bar{K}+1)+2$
Number of links	$2^{X_J}M(X_R+1)X_L$	$X_N(\bar{K}+2)+X_L[2(\bar{K}+1)-X_W](X_W+1)-2(X_W+1)\sum_h t_h^0$	$X_1(\bar{K}+2)+\sum_{d\neq d',\, d,d'\in D} N_{d,d'}$

The mathematical expressions of the number of nodes and links of the supernetwork representation for the multi-state supernetwork approach and the activity-time supernetwork (ATS) approach are summarised in *Table 2*. The following notations are employed, where X_N is the number of nodes in the basic transportation network $\bar{G}$, X_L is the number of links in $\bar{G}$, X_J is the number of types of activities in $\bar{G}$, and M is the number of user classes. Note that $X_J \leq X_1$, since one activity can be conducted in different location nodes. For the multi-state supernetwork approach X_R is used to denote the number of parking locations in $\bar{G}$, whereas for the ATS approach X_W is used to denote the maximum tolerable queuing time in $\bar{G}$, which is expressed as an integer multiplier of T_L.

Recall that the calculation of the number of nodes and links of AJN is mainly described in Section 2.1. Here we briefly introduce the derivation of the number of nodes and links of the supernetwork representation for the other two approaches.

For the multi-state supernetwork approach, the supernetwork is composed of one public transport network and multiple private vehicle networks for individual users, which are interconnected by the transition links between parking locations and public transport stops/stations. When the number of types of activities in $\bar{G}$ is X_J, the supernetwork has 2^{X_J} possible activity states, and for each activity state there are at least X_R+1 possible vehicle states. In total, the multi-state supernetwork representation needs $2^{X_J}(X_R+1)$ copies of $\bar{G}$ for a given class of users, and thus the number of nodes and links in the resulting supernetwork are $2^{X_J}(X_R+1)X_N$ and $2^{X_J}(X_R+1)X_L$, respectively. Moreover, when there are multiple classes of users with different home locations in $\bar{G}$ and/or different preferences of activity agendas, the multi-state supernetwork approach needs to generate a separate supernetwork for each class of users.

For the ATS approach, each node in $\bar{G}$ is augmented into $\bar{K}+1$ nodes along the time dimension, and activity links are generated between these augmented nodes of that node indicating the cases where an activity is conducted at that node and lasting for one time interval. Thus, the number of nodes and links in the ATS which are generated from the *nodes* in $\bar{G}$ are $X_N(\bar{K}+1)$ and $X_N\bar{K}$, respectively. On the other hand, each link in $\bar{G}$ is expanded to multiple travel links and queuing links, where travel links represent the possible movement of users between different nodes with a feasible departure time, and queuing links illustrate the one-time-interval queuing behaviour of users when link flow exceeds link capacity. Specifically, for a link h in $\bar{G}$ the number of the feasible set of departure time is $\bar{K}+1-t_h^0$, where t_h^0 is the free-flow travel time of link h. Thus, the number of travel links and queuing links generated from a link h in $\bar{G}$ are $\bar{K}+1-t_h^0$ and $(\bar{K}+1-t_h^0-X_W)X_W+\frac{X_W(X_W-1)}{2}$, respectively. Exit links are generated to show the processes that users exit travel links or queuing links, and thus the number of exit links is the sum of the number of travel links and queuing links. An equivalent number of nodes are needed to indicate these expanded links. As a result, from a link h in $\bar{G}$ the number of expanded nodes and links in ATS are $(\bar{K}+1-t_h^0-X_W)(X_W+1)+\frac{X_W(X_W+1)}{2}$ and $2(\bar{K}+1-t_h^0-X_W)(X_W+1)+X_W(X_W+1)$, respectively. When the number of links in $\bar{G}$ is X_L, the number of nodes and links in the ATS which are generated from the *links* in $\bar{G}$ are $X_L(\bar{K}+1-0.5X_W)(X_W+1)-(X_W+1)\sum_h t_h^0$ and $X_L[2(\bar{K}+1)-X_W](X_W+1)-2(X_W+1)\sum_h t_h^0$, respectively. Finally, the ATS also contains one dummy start node, one dummy end node, X_N start links and X_N end links.

It can be seen from *Table 2* that the AJN approach develops a simpler supernetwork representation in terms of network size for dealing with the dynamic activity-travel scheduling problem in a transportation network when compared with the multi-state supernetwork approach and the ATS approach. The total number of nodes and links of the multi-state supernetwork increase exponentially with the number of activities X_J, whereas those of the activity-time supernetwork and the activity-journey-network both increase in a polynomial manner. Note that computational efforts expended on solving the dynamic activity-travel scheduling problem are mainly required by identifying the maximum-utility path (or the equivalent minimum-travel-time path) in each iteration, which depends heavily on the number of nodes and links of the supernetwork representation. Thus, the development of a simpler supernetwork representation can facilitate us to better analyse and solve the related dynamic activity-travel scheduling problem.

By applying the results of *Table 2*, *Table 3* lists the number of nodes and links for the expansion of the small network (in numerical example 1), the Sioux Falls network and the Anaheim network through the multi-state supernetwork approach, ATS approach and AJN approach, respectively. The values of parameters used in the calculation are set as follows: (1) for the small transportation network in numerical example 1 (see *Figure 1*), $X_N=5$, $X_L=16$, $X_J=4$, $X_1=5$, $M=2$, $\bar{K}=144$, $X_R=4$ and $X_W=6$; (2) for the Sioux Falls network, $X_N=24$, $X_L=76$, $X_J=4$, $X_1=5$, $M=2$, $\bar{K}=144$, $X_R=5$ and $X_W=6$; and (3) for the Anaheim network, $X_N=416$, $X_L=914$, $X_J=4$, $X_1=5$, $M=2$, $\bar{K}=360$, $X_R=5$ and $X_W=60$. The determination of the value of X_R is based on [22] where activity locations should be all considered as potential parking locations, while the value of X_W is given according to the length of a time interval and the maximum tolerable queuing time, which is set to be 1 hour here for illustration purposes.

Table 3 – Comparison of network size in the expanded multi-state supernetwork, ATS and AJN

Type of networks		Multi-state supernetwork	ATS	AJN
Small network	Number of nodes	800	16,421	727
	Number of links	2,560	32,118	3,590
Sioux Falls network	Number of nodes	4,608	78,326	727
	Number of links	14,592	153,192	3,572
Anaheim network	Number of nodes	79,872	18,537,347	1,807
	Number of links	175,488	36,924,930	8,875

It can be seen from *Table 2-3* that with the increase of a number of activities X_J (as well as the number of activity location nodes X_1), the gap of expanded network size between AJN and other approaches will grow dramatically. We will show how large this gap can be through a simple example. For the Anaheim network, imagine the scenario that all the 38 zones in this network can serve as activity locations and each zone can conduct one single type of activity, thus the value of X_J is 38. Calculating the number of nodes and links of the supernetwork representation for the multi-state supernetwork approach, the ATS approach and the AJN approach with setting $X_J=X_1=38$ and remaining the value of the rest parameters, as shown in *Table 4*, it is clear to see the difference in the magnitude of network size of the supernetwork representation among these three approaches is significant.

Table 4 – Sizes of the expanded multi-state supernetwork, ATS and AJN of Anaheim network

		Multi-state supernetwork	**ATS**	**AJN**
Anaheim network (one activity feasible at one zone, and a total of 38 zones)	**Number of nodes**	4.46×10^{15}	1.85×10^{7}	1.37×10^{4}
	Number of links	9.80×10^{15}	3.69×10^{7}	5.21×10^{5}

4. CONCLUSION

In this paper, we study the multi-class user activity-travel scheduling problem under time constraints. A simple supernetwork representation approach is introduced to expand the basic transportation network in both time and space dimensions. The network size of the supernetwork representation in terms of number of nodes and links is analysed and compared with other approaches, which exhibits a significant reduction in the magnitude of the network size of the supernetwork representation, especially for the cases with a larger number of activities/activity locations. With the supernetwork representation, the dynamic activity-travel scheduling problem is transformed into a static network flow assignment problem. An activity-based multi-class user equilibrium model is formulated on the expanded AJN. A heuristic algorithm is developed to find the path with the maximum utility in the AJN from the start node to the end node for each user. A numerical study is conducted to illustrate the application of the proposed model and solution algorithm for dealing with real-world transportation networks. The computational results show that network users' travel behaviours including activity choices and travel choices are well studied, which facilitates us to better understand network users' travel behaviour, and make transport and urban land use policies more properly.

Future research to be carried out may include: (*a*) refining the proposed AJN approach to incorporate the consideration of physical queuing problems both on transport links and at activity location nodes, (*b*) studying the activity and travel choice behaviour in a multimodal transportation network, and (*c*) developing advanced methods with new techniques to discuss the interdependence among users' activity and travel choices.

ACKNOWLEDGEMENTS

The authors are extremely grateful to the editor and the anonymous reviewers for their valuable comments and suggestions on continuously improving the quality of this work. This paper was supported by the National Natural Science Foundation of China (grant no. 71971020) and the Doctoral Innovation Research Fund of Tangshan University.

REFERENCES

[1] Golob TF. Structural equation modeling for travel behavior research. *Transportation Research Part B*. 2003;37:1-25. DOI: 10.1016/S0191-2615(01)00046-7.

[2] Di X, Liu HX. Boundedly rational route choice behavior: A review of models and methodologies. *Transportation Research Part B*. 2016;85:142-179. DOI: 10.1016/j.trb.2016.01.002.

[3] Ahmad F, Al-Fagih L. Travel behaviour and game theory: A review of route choice modeling behaviour. *Journal of Choice Modelling*. 2024;50:1-34. DOI: 10.1016/j.jocm.2024.100472.

[4] Zang Z, et al. Travel time reliability in transportation networks: A review of methodological developments. *Transportation Research Part C*. 2021;131:103334. DOI: 10.1016/j.trc.2022.103866.

[5] Johari M, et al. Macroscopic network-level traffic models: Bridging fifty years of development toward the next era. *Transportation Research Part C*. 2022;143:103866. DOI: 10.1016/j.trc.2021.103334.

[6] Mukherjee J, Kadali BR. A comprehensive review of trip generation models based on land use characteristics. *Transportation Research Part D*. 2022;109:103340. DOI: 10.1016/j.trd.2022.103340.

[7] Mariotte G, et al. Macroscopic urban dynamics: analytical and numerical comparisons of existing models. *Transportation Research Part B*. 2017;101:245-267. DOI: 10.1016/j.trb.2017.04.002.

[8] Gu Z, et al. Macroscopic parking dynamics and equitable pricing: Integrating trip-based modeling with simulation-based robust optimization. *Transportation Research Part B*. 2023;173:354-381. DOI: 10.1016/j.trb.2023.05.011.

[9] Zhong R, et al. Dynamic user equilibrium for departure time choice in the basic trip-based model. *Transportation Research Part C*. 2021;128:103190. DOI: 10.1016/j.trc.2021.103190.

[10] Ettema DF, Timmermans HJ. *Activity-based approaches to travel analysis*. New York, USA: Pergamon; 1997.

[11] Li ZC, et al. Bottleneck model revisited: An activity-based perspective. *Transportation Research Part B*. 2014;68:262-287. DOI:10.1016/j.trb.2014.06.013.

[12] Li ZC, et al. Step tolling in an activity-based bottleneck model. *Transportation Research Part B*. 2017;101:306-334. DOI:10.1016/j.trb.2017.04.001.

[13] Li ZC, et al. Fifty years of the bottleneck model: A bibliometric review and future research directions. *Transportation Research Part B*. 2020;139:311-342. DOI: 10.1016/j.trb.2020.06.009.

[14] Yu X, et al. Autonomous cars and activity-based bottleneck model: How do in-vehicle activities determine aggregate travel patterns? *Transportation Research Part C*. 2022;139:103641. DOI: 10.1016/j.trc.2022.103641.

[15] Lee MS, McNally MG. On the structure of weekly activity/travel patterns. *Transportation Research Part A*. 2003;37:823-839. DOI: 10.1016/S0965-8564(03)00047-8.

[16] Rasouli S, Timmermans H. Effects of travel time delay on multi-faceted activity scheduling under space-time constraints: A simulation study. *Travel Behaviour and Society*. 2014;1:31-35. DOI: 10.1016/j.tbs.2013.10.002.

[17] Li Q, et al. Incorporating free-floating car-sharing into an activity-based dynamic user equilibrium model: A demand-side model. *Transportation Research Part B*. 2018;107:102-123. DOI: 10.1016/j.trb.2017.11.011.

[18] Nguyen TK, et al. A unified activity-based framework for one-way car-sharing services in multi-modal transportation networks. *Transportation Research Part E*. 2022;157:102551. DOI: 10.1016/j.tre.2021.102551.

[19] Fu X, et al. An activity-based model for transit network design and activity location planning in a three-party game framework. *Transportation Research Part E*. 2022;168:102939. DOI: 10.1016/j.tre.2022.102939.

[20] Dianat L, et al. Modeling and forecasting daily non-work/school activity patterns in an activity-based model using skeleton schedule constraints. *Transportation Research Part A*. 2020;133:337-352. DOI: 10.1016/j.tra.2020.01.017.

[21] Chen S, et al. Formulation and solution approach for calibrating activity-based travel demand model-system via microsimulation. *Transportation Research Part C*. 2020;119:102650. DOI: 10.1016/j.trc.2020.102650.

[22] Liao F, et al. Constructing personalized transportation network in multi-state supernetworks: A heuristic approach. *International Journal of Geographic Information Science*. 2011;25(11):1885-1903. DOI: 10.1080/13658816.2011.556119.

[23] Liao F, et al. Supernetwork approach for modeling traveler response to park-and-ride. *Transportation Research Record: Journal of the Transportation Research Board*. 2012;2323 (1):10-17. DOI: 10.3141/2323-02.

[24] Liao F, et al. Incorporating space-time constraints and activity-travel time profiles in a multi-state supernetwork approach to individual activity-travel scheduling. *Transportation Research Part B*. 2013;55:41-58. DOI: 10.1016/j.trb.2013.05.002.

[25] Liao F, et al. Effects of land-use transport scenarios on travel patterns: A multi-state supernetwork application. *Transportation*. 2017;44:1–25. DOI: 10.1007/s11116-015-9616-z.

[26] Liu P, et al. Dynamic activity-travel assignment in multi-state supernetworks. *Transportation Research Part B*. 2015;81:656–671. DOI: 10.1016/j.trpro.2015.06.002.

[27] Liu P, et al. Day-to-day needs-based activity-travel dynamics and equilibria in multi-state supernetworks. *Transportation Research Part B*. 2020;132:208-227. DOI: 10.1016/j.trb.2019.05.017.

[28] Ouyang LQ, et al. Network user equilibrium model for scheduling daily activity travel patterns in congested networks. *Transportation Research Record: Journal of the Transportation Research Board*. 2011;2254:131- 139. DOI: 10.3141/2254-14.

[29] Fu X, Lam WHK. A network equilibrium approach for modelling activity-travel pattern scheduling problems in multi-modal transit networks with uncertainty. *Transportation*. 2014;41(1):37-55. DOI: 10.1007/s11116-013-9470-9.

[30] Fu X, Lam WHK. Modelling joint activity-travel pattern scheduling problem in multi-modal transit networks. *Transportation*. 2018;45(1):23-49. DOI: 10.1007/s11116-016-9720-8.

[31] Voa KD, et al. A household optimum utility approach for modeling joint activity-travel choices in congested road networks. *Transportation Research Part B*. 2020;134: 93–125. DOI: 10.1016/j.trb.2020.02.007.

[32] Lin X, et al. Formulating multi-class user equilibrium using mixed-integer linear programming. *EURO Journal on Transportation and Logistics*. 2022;11, [100097]. DOI: 10.1016/j.ejtl.2022.100097.

[33] Ameli M, et al. Computational methods for calculating multimodal multiclass traffic network equilibrium: Simulation benchmark on a large-scale test case. *Journal of Advanced Transportation*. 2021;3:1-17. DOI: 10.1155/2021/8815653.

[34] Nagurney A, Dong J. A multiclass, multicriteria traffic network equilibrium model with elastic demand. *Transportation Research Part B*. 2002;36(5):445-469. DOI: 10.1016/S0191-2615(01)00013-3.

[35] Nagurney A. A multiclass, multicriteria traffic network equilibrium model. *Mathematical and Computer Modeling*. 2000;32(3–4):393–411. DOI: 10.1016/S0895-7177(00)00142-4.

[36] Kontar W, et al. On multi-class automated vehicles: Car-following behavior and its implications for traffic dynamics. *Transportation Research Part C*. 2021;128,[103166]. DOI: 10.1016/j.trc.2021.103166.

[37] Hamadneh J, Esztergár-Kiss D. Potential travel time reduction with autonomous vehicles for different types of travellers. *Promet-Traffic & Transportation*. 2021;33(1):61-76. DOI: 10.7307/PTT.V33I1.3585.

[38] Gim THT. Analysing the effects of land use on the choice of intra-zonal trip destinations-a comparison between weekday and weekend travel. *Promet-Traffic & Transportation*. 2020;32(4):527-542. DOI: 10.7307/PTT.V32I4.3399.

[39] Daisy NS, et al. Modeling activity-travel behavior of non-workers grouped by their daily activity patterns. In: Goulias KG, Davis AW. (eds) *Mapping the travel behavior genome*. Cambridge, MA, United States: Elsevier; 2020. p. 339-370.

[40] Ettema D, Timmermans HJP. Modeling departure time choice in the context of activity scheduling behaviour. *Transportation Research Record: Journal of the Transportation Research Board*. 2003; 1831:39-46. DOI: 10.3141/1831-05.

[41] Transportation Networks for Research Core Team. Transportation Networks for Research. https://github.com/bstabler/TransportationNetworks. Accessed: 2024-07-15.

欧阳恋群，黄帝，肖玲玲

出行时间约束下交通网络多类型用户出行行为的活动-行程-网络建模方法

摘要
交通网络中用户的出行决策决定了实时的交通流量形态，而这些出行决策又是基于用户的一些活动意图而制定的，例如外出工作、就餐、购物等。因此，用于准确描述用户活动选择和出行行为之间相互作用关系的模型构建方法是交通管理规划的重要基石。在本论文中提出了一个用来研究出行时间约束下多用户活动-出行计划的基于活动的交通网络用户均衡模型，并介绍了一种简便的超网络建模方法。通过将原始交通网络在时间维度和空间维度进行拓展，可以得到一个超网络。在该超网络中，动态的活动-出行规划决策问题能够被转换为静态的网络配流问题，进而可以设计出启发式求解算法，为每位网络用户找出出行效用最大化的最优路径。在数值实验中，本论文所提出的模型和算法被应用于若干个交通网络（包括大型真实的城市交通路网），结果表明，无论是交通网络中单个用户的出行选择还是群体出行行为均能够得到很好地分析和研究。

关键词
活动-出行计划；活动出行网络；超网络；出行行为；多类型用户；时间约束